Toxicology and Applied Pharmacology 274 (2014) 339–349

Contents lists available at ScienceDirect

Toxicology and Applied Pharmacology

journal homepage: www.elsevier.com/locate/ytaap

Developmental defects in zebrafish for classification of EGF pathway inhibitors☆

Benoist Pruvot, Yoann Curé, Joachim Djiotsa, Audrey Voncken, Marc Muller *

Laboratory for Organogenesis and Regeneration, Université de Liège, GIGA-R B34, Sart Tilman, 4000 Liège, Belgium

ARTICLE INFO

Article history:
Received 30 September 2013
Revised 5 November 2013
Accepted 7 November 2013
Available online 18 November 2013

Keywords:
Zebrafish
Epidermal growth factor
Cartilage
Vascular
Drug testing
Myelin

ABSTRACT

One of the major challenges when testing drug candidates targeted at a specific pathway in whole animals is the discrimination between specific effects and unwanted, off-target effects. Here we used the zebrafish to define several developmental defects caused by impairment of Egf signaling, a major pathway of interest in tumor biology. We inactivated Egf signaling by genetically blocking Egf expression or using specific inhibitors of the Egf receptor function. We show that the combined occurrence of defects in cartilage formation, disturbance of blood flow in the trunk and a decrease of myelin basic protein expression represent good indicators for impairment of Egf signaling. Finally, we present a classification of known tyrosine kinase inhibitors according to their specificity for the Egf pathway.

In conclusion, we show that developmental indicators can help to discriminate between specific effects on the target pathway from off-target effects in molecularly targeted drug screening experiments in whole animal systems.

Introduction

During the past decades, molecularly targeted therapies for various diseases have been developed, offering a more rational approach than classical drug development due to a higher efficiency against the drug target combined with minimized secondary effects. Although biochemical or cell-based assays are efficient at detecting pathway-specific drugs, whole animal systems are more reliable for detection of unwanted side effects. Toxicity of such targeted drugs may result from off-target effects due to lack of specificity, but also from specific effects due to inhibition of the intended target also required in healthy cells (Gibbs, 2000). For example, inhibition of gamma-secretase for treatment of Alzheimer's disease will also affect Notch signaling (Bulic et al., 2011). Similarly, inhibition of the Egfr pathway for cancer therapy leads to skin rash after two weeks due to Egfr inhibition (Li and Perez-Soler, 2009). Although unwanted, such a mechanism-based toxicity is however useful as evidence for specific pathway inactivation (Dienstmann et al., 2011). Moreover, while observed lethality or teratogenicity might in general exclude a tested compound for direct clinical application, the detection of specific effects could however qualify it for investigation of related molecules that could decrease the unwanted side effects. Thus, one of the major challenges when screening for new compounds affecting specific pathways in a whole animal model such as zebrafish is the discrimination between specific effects on the targeted pathway and more general off-target effects.

In the field of tumor biology, the Epidermal Growth Factor (EGF) pathway has been a preferred target for inhibition due to its involvement in a wide variety of cancer types (Bianco et al., 2007; Eccles, 2011; Harari et al., 2007; Shilo, 2003; Sibilia et al., 2007). The EGF ligand family consists of one member in *Caenorhabditis elegans* (Chang and Sternberg, 1999), five in *Drosophila melanogaster* and ten in vertebrates (Olayioye et al., 2000; Yarden and Sliwkowski, 2001), while the EGF receptor belongs to a family of four receptors in humans. The latter includes EGF receptor (EGFR), also known as ErbB1 or HER1 (Human EGF Receptor 1), ErbB2/neu/HER2, ErbB3/HER3 and ErbB4/HER4 (Olayioye et al., 2000; Yarden and Sliwkowski, 2001). Similar to other ErbB members, EGFR is a 170 kDa glycoprotein containing a cystein-rich extracellular ligand binding domain, a hydrophobic transmembrane domain and a cytoplasmic tyrosine kinase domain. In mammals, a large variety of ligands are recognized by ErbB members that can form homo- or heterodimers and consequently, ErbB signaling displays a remarkable diversity (Holbro and Hynes, 2004; Seshacharyulu et al., 2012).

EGFs and their receptors are regulators of cell proliferation, differentiation, survival, motility, and apoptosis (Olayioye et al., 2000; Yarden and Sliwkowski, 2001). Moreover, their involvement in many normal physiological processes such as embryonic tissue development, skin (Luetteke et al., 1994; Pastore et al., 2008), kidney (Zeng et al., 2009), mammary gland (Hardy et al., 2010), heart (Iwamoto and Mekada, 2006) lung, intestine, myelination (Aguirre et al., 2007), craniofacial skeleton (Miettinen et al., 1999; Sibilia et al., 2003; Wang et al., 2004) confer a key regulatory role to the EGF pathway. EGFR

* Corresponding author. Fax: +32 4 366 4198.
E-mail address: m.muller@ulg.ac.be (M. Muller).

0041-008X/$ – see front matter © 2013 The Authors. Published by Elsevier Inc. All rights reserved.
http://dx.doi.org/10.1016/j.taap.2013.11.006

signaling was previously shown to be involved in cartilage (Fisher et al., 2007; Pan et al., 2011; Saito et al., 2013; Shum et al., 1993; Takeda et al., 2010) and bone (Schneider et al., 2009; Wang et al., 2004; Zhang et al., 2011; Zhu et al., 2011) development. Disruption of this pathway also revealed its involvement in renal pathologies (Zeng et al., 2009), bone pathologies (Schneider et al., 2009), bone metastasis (Lu and Kang, 2010) or skin inflammation (Pastore et al., 2008). Amplification and inappropriate activation of EGF receptor family members are associated with tumor growth (Blume-Jensen and Hunter, 2001; Hardy et al., 2010; Yarden and Sliwkowski, 2001), psoriasis (Jost et al., 2000) or cardiomyopathy (Asakura et al., 2002; Crone et al., 2002). In particular, its potential as a target for anti-tumor drug development (Seshacharyulu et al., 2012) triggered research to inhibit EGFR function using various approaches such as monoclonal antibodies (cetuximab and panitumumab) or tyrosine kinase inhibitors (TKI, erlotinib or gefitinib) (Harari et al., 2007; Langer, 2007; Maccari et al., 2007; Scaltriti and Baselga, 2006). Numerous protein tyrosine kinase inhibitors, named tyrphostins (TYRosine PHOSphorylation Inhibitors) naturally exist, such as quercetin, genistein, erbstatin or lavendustin, which inhibit Ser/Thr kinases and several other enzymes, but were found to have a low specificity for EGFR. To enhance their specificity, synthetic tyrphostins have been developed. The anilinoquinazoline AG-1478 was found to reversibly inhibit EGFR with high specificity (Barker et al., 2001) and efficacy in liver tumors (Caja et al., 2011), laryngeal cancers (Kang et al., 2010) and glioblastoma (Carrasco-Garcia et al., 2011).

Although few studies have been carried out in zebrafish and medaka, two copies of EGFR (*egfra* and *egfrb*) genes have been described in teleosts (Laisney et al., 2010; Morizot et al., 1998). Compared to humans, an 89% protein sequence similarity is observed in the intracellular kinase domains, while the extracellular domains of zebrafish Egfrs are less conserved (58% similarity). Expression of *egfr1a* was shown to be ubiquitous in adults (Wang and Ge, 2004). Four zebrafish homologs for members of the Egf ligand family (*egf*, *btc*, *tgfα*, *hb-egf*) have been isolated (Laisney et al., 2010; Tse and Ge, 2009) and their expression in adults was evaluated. All four exhibited ubiquitous expression, except that *egf* was absent from gills and pituitary. In female gonads, expression of all four ligands was detected in the oocyte, whereas *egfr1* was only found in the follicular layer (Tse and Ge, 2009). Expression of *hb-egf*, *egf* and *btc* was detected by *in situ* hybridization in the retina (Wan et al., 2012). Three additional members (Areg, Ereg and Epgn) have been identified (Laisney et al., 2010), but no information on their expression pattern is available to date. In zebrafish, EGFR signaling is involved in cardiovascular development (Goishi et al., 2003) and in oocyte maturation (Pang and Ge, 2002; Wang and Ge, 2004), disruption of *hb-egf* expression leads to myocardial contractile dysfunction (Friedrichs et al., 2009). The specific inhibitor AG-1478 was also shown to have an effect on blood vessel development in a chemical screening experiment using a transgenic *vegfr2-GFP* line expressing GFP in the blood vessels (Tran et al., 2007).

Many investigations into the role of Egf signaling are based on the study of its receptor Egfr/ErbB1. Here, we concentrate on the biological functions of the Egf pathway by determining the effect of Egf depletion on developing zebrafish during the first 4 days and comparing these defects to those observed upon inhibition of Egfr function.

Materials and methods

Substances. AG-18, AG-213, AG-490, AG-825 and AG-1478 were purchased from Tocris (Bristol, UK). Stock solutions were prepared by dissolving the pure chemicals in DMSO and then diluted to the desired concentrations in E3 medium. Final DMSO concentrations were <1% in the final solution. Effects of DMSO alone were evaluated at 1%, the maximum concentration used during the assays.

Zebrafish maintenance. Adult strain AB zebrafish (ZIRC, Eugene, OR) were kept at 28 °C as described (Westerfield, 2007). The light:dark cycle was 14:10 h. Wild-type fish were mated and spawning was stimulated by the onset of light. Then, eggs were collected and placed at 28 °C in Petri dishes containing E3 medium (5 mM NaCl, 0.17 mM KCl, 0.4 mM CaCl2, and 0.16 mM MgSO4). Embryos and larvae were staged according to Kimmel et al. (Kimmel et al., 1995). The age of the embryos and larvae is indicated as hours post fertilization (hpf) or days post fertilization (dpf). Animal care and all experimentation were conducted in compliance with Belgian and European laws (Authorization: LA1610002, Ethical commission protocols ULg1076 and ULg624).

Drug treatment and larvae observation. Treatments were administered to 4 hpf zebrafish larvae distributed in pools of 25 into 6 well plates in E3 medium. The treatment solution was renewed every 24 h. All experiments were carried out at least in duplicate on $n = 25$ larvae per test and repeated at least three times. Survival and morphological or developmental defects were assessed every day from 1 dpf to 4 dpf using an Olympus SZX10 stereomicroscope coupled with an Olympus XC50 camera. To assess teratogenicity, the surviving larvae were observed for morphological defects and the number of larvae presenting at least one morphological defect was reported as percentage of the surviving larvae. For calculation of LC50, LC10, EC50 and EC10 values, the Graphpad software was used. The teratogenic index (TI), defined as the ratio between LC_{50} and EC_{50}, was calculated; a substance is considered to be teratogenic when $TI > 1$, and considered as producing embryo lethal effects when $TI \leq 1$.

Whole mount in situ hybridization (WISH). Whole mount *in situ* hybridization was performed as previously described (Hauptmann and Gerster, 2000) using an Insitu Pro VSi robot (Intavis, Koeln, Germany). Antisense RNA probes were synthesized by transcription of cDNA clones with T7, T3 or SP6 RNA polymerase using digoxigenin labeling mix (Roche Applied Science). Treated and non-treated larvae were fixed 4 days post fertilization (4 dpf) in PFA 4%. *In situ* labeling was observed using an Olympus SZX10 stereomicroscope coupled with an Olympus XC50 camera.

Alcian blue staining. Cartilage was stained with Alcian Blue 8 GX (Sigma®) as previously described (Dalcq et al., 2012). Briefly, four days old larvae were fixed in PFA 4% for 2 h at room temperature, rinsed with PBST and finally stained overnight with 10 mM MgCl2/80% ethanol/0.04% Alcian Blue solution. Embryos were rinsed with 80% ethanol/10 mM MgCl2. Pigments were bleached in H2O2 3%/KOH 0.5% for 1 h.

Morpholino antisense knock down analysis. A morpholino oligonucleotide (MO) was synthesized by Gene Tools (Philomath, OR, USA) that is complementary to the splice donor site of exon 4. MO stock solutions were prepared as suggested by Gene Tools. Tetramethylrhodamine dextran (Invitrogen, Belgium) was added at a concentration of 0.5% to sort correctly injected embryos a few hours after injection. The MOegf morpholino sequence is: 5′-AAGAGAAACCGAGGCTGTACCTTCA-3′.

Reverse transcription and real-time PCR analysis. Total RNA from pools of 100 treated or control larvae was isolated with Trizol (Invitrogen, Cergy Pontoise, France) using the RNeasy extraction kit (Qiagen, Venlo, Netherlands) and reverse transcribed by Moloney murine leukemia virus reverse transcriptase (Promega, Madison, WI) using random hexamer primers (Promega, Madison, WI). At least three pools were analyzed for each treatment and the corresponding control. Real-time quantitative PCR (qPCR) was performed with AmpliTaq Gold polymerase in an Applied Biosystem 7500 Fast thermocycler using the standard SyBr Green detection protocol (Applied Biosystems, Foster City, CA). Briefly, 12 ng of total cDNA, 50nM (each) primers, and 1× SyBr Green mixture were used in a total volume of 20 μL. The results were analyzed using the β-actin cDNA amplification as internal standard and fold-change was

calculated relative to untreated control using the ΔΔCt method (Pfaffl, 2001). qPCR analysis on each RNA sample was performed in triplicate and one representative result out of at least three independent experiments is shown.

The following PCR primers were used: *β-actin*: 5′-CAGACATCA GGGAGTGATGG-3′ (forward) and 5′-ATGGGGTATTTGAGGGTCAG-3′ (reverse); *mbp*: 5′-CCGTCGTGGAGACGTCAA-3′ (forward) and 5′-CG AGGAGAGGACACAAAGCT-3′ (reverse).

Microangiography. Microangiography was performed by injecting isolectine GS-IB4 Alexa Fluor 568 conjugate (Invitrogen, Gent, Belgium) into the *sinus venosus* of 4 dpf larvae. Injected larvae were observed using an Olympus SZX10 stereomicroscope coupled with an Olympus XC50 camera.

Statistical analysis. All statistical analyses were performed using Graphpad prism for Windows (version 5.03). LC50, LC10, EC50 and EC10 were calculated by plotting the surviving/affected larvae against the log transformed tested concentration and the obtained curve was fitted to a sigmoid concentration-response relation according to the following equation: $Y = \text{Bottom} + (\text{Top–Bottom}) / (1 + 10^{(\log EC50 - x)})$ where bottom and top represent respectively the lowest and the highest y-value (% survivors/affected). The resulting calculated logEC/LC were extracted and their corresponding SD given (Table 5).

The decrease/increase in gene expression as determined by qPCR was analyzed using one-way ANOVA followed by Dunnett's multiple comparison test (Steel and Torrie, 1996). Significance was considered when P values were lower than 0.05. (***) indicates statistical significance $P < 0.005$ (**) $P < 0.01$ (*) $P < 0.05$. The results are expressed as mean plus or minus SD.

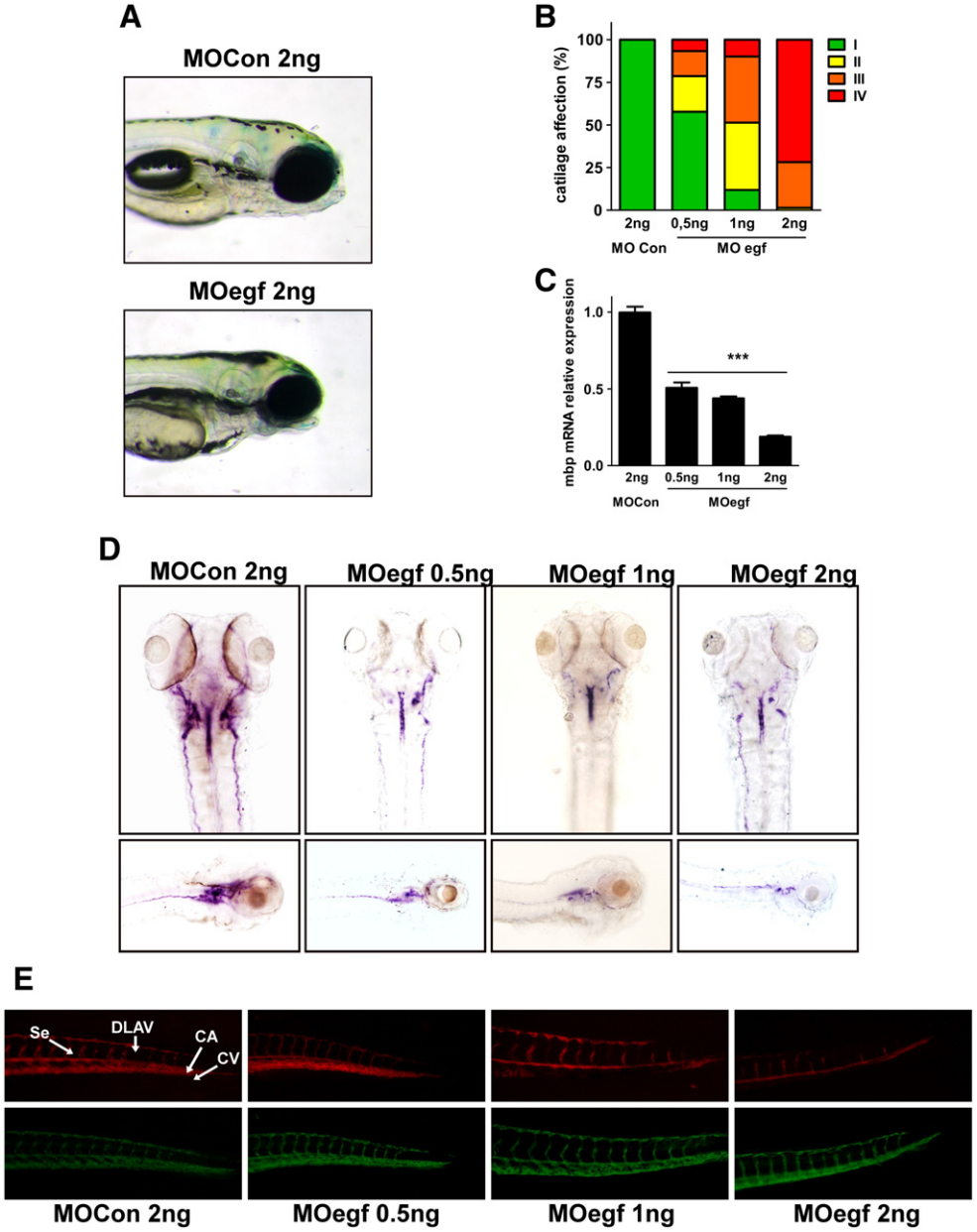

Fig. 1. Developmental defects as a result of *egf* knock down in 96 hpf zebrafish embryos. (A) Observable impairment of mandibular tissues in 96 hpf morphants. (B) Proportions of head cartilage patterns in control and morphants (I. no observable defect; II. Shortened Meckel's cartilage; III. Shortened Meckel's cartilage and attenuated or absent ceratobranchials and IV. No cartilage formation). (C) Myelin basic protein expression analyzed by whole mount *in situ* hybridization or (D) qPCR. Effects of Egf depletion on trunk vessel formation by microangiography (E) in transgenic fli-GFP embryos. A: aorta; CV: Cardinal vein; DLAV: Dorsal longitudinal anastomotic vessel and Se: intersegmental vessels.

Results

Developmental defects caused by inhibition of EGF expression

To define the developmental defects caused by inhibition of EGF signaling, we decided to perform genetic knock-down of the Egf pathway. In zebrafish, two homologs have been described for the human EGF receptor gene (*egfra* and *egfrb*), while only one gene is found coding for Egf (Laisney et al., 2010). Thus, we decided to genetically inhibit expression of the endogenous *egf* gene by microinjection of a specific antisense morpholino oligonucleotide targeting the splice donor site of exon 4 into the one-cell stage embryo.

In a first exploratory experiment, injection of 2 ng of MOegf led to 6% mortality at 4 dpf, while no occurrence of morphological defects or necrosis was observed. Close inspection of 4 dpf *egf* morphants revealed an apparent absence of ventral tissue in the anterior head region, presumably the mandibular cartilage (Fig. 1A). This effect was further characterized by microinjection of various amounts of MOegf. Morpholino-injected and control embryos were analyzed by alcian blue staining for the cartilage extracellular matrix. Four different head cartilage patterns were observed on those larvae (Fig. 2): type I with no observable defect; type II presenting shortened Meckel's cartilage; type III with shortened Meckel's cartilage associated with attenuated or absent ceratobranchials and type IV without any cartilage formation. While 0.5 ng MOegf caused weak cartilage defects (type II) in 20% and more severe (type III and IV) in 22% of the observed larvae, injection of 1 ng led to a higher proportion of type II defects (39%), type III (39%) and type IV (10%) cartilage defects in morphants. Finally, injection of 2 ng of MOegf led to type III malformations in 27% and to severe type IV defects in 72% of injected larvae (Table S1, Fig. 1B).

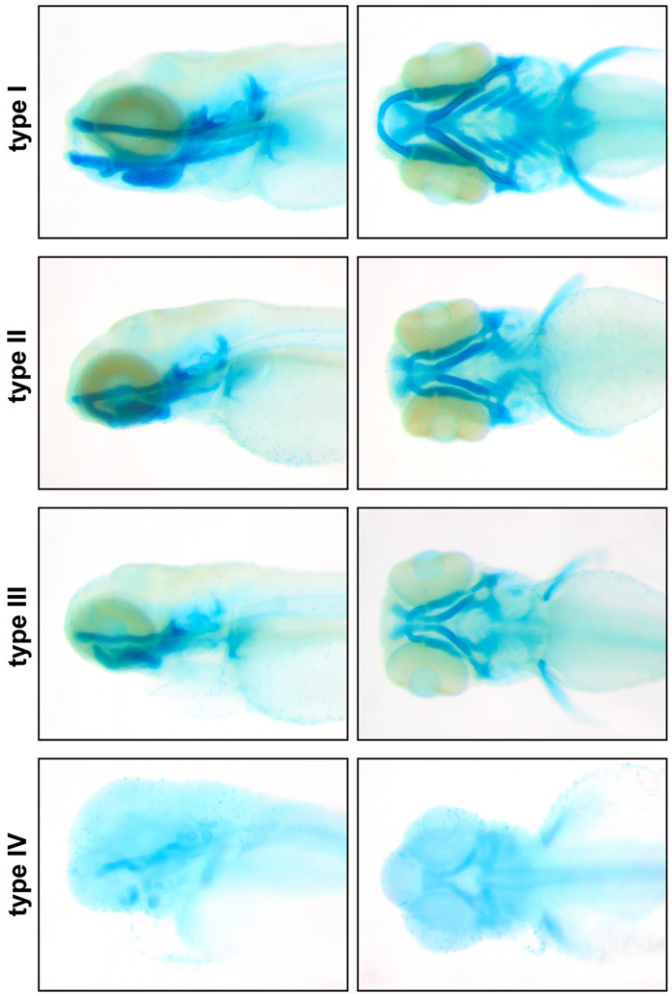

Fig. 2. Observed head cartilage patterns. Observable head cartilage patterns stained with alcian blue in 4 dpf embryos upon Egf pathway disruption. Type I: no observable defect; type II: shortened Meckel's cartilage; type III: shortened Meckel's cartilage associated with attenuated or absence of ceratobranchials and type IV: without any cartilage formation.

We also determined the effect of Egf knock down on myelin formation. Myelin basic protein (Mbp) is one of the major components of myelin both in the central and peripheral nervous system. *In situ* hybridization of 4 dpf control embryos revealed *mbp* expression in the midbrain–hindbrain, the oligodendrocytes of the anterior lateral line (ALL) and in the medial longitudinal fascicle bifurcating rostrally into cranial nerves. In MOegf morphants, a dose dependant decrease of *mbp* expression was clearly observed (Fig. 1D). Quantitative analysis by RT-PCR on total mRNA revealed a 2-fold, 3-fold and 5-fold decrease of *mbp* mRNA levels upon injection of, respectively 0.5, 1 or 2 ng of MOegf relative to larvae previously injected with a control morpholino (Fig. 1C).

Finally, we investigated the effect of Egf depletion on trunk vessel formation and function. We performed micro-angiography on transgenic *fli1-GFP* embryos in order to compare the presence of the green fluorescent blood vessels to the blood flow visualized by the red fluorescence of previously microinjected isolectine GS-IB4 Alexa Fluor 568. In control larvae (MOCon 2 ng), the aorta (A), the cardinal vein (CV), the dorsal longitudinal anastomotic vessel (DLAV) and the intersegmental (Se) vessels were clearly distinguished (green) and blood circulation was observed in all these vessels (Fig. 1E). Larvae injected with MOegf exhibited clear circulation defects, while the blood vessels appeared to be correctly formed. At 1 ng of morpholino, the larvae were characterized by a lack of circulation in the caudal vein (CV), dorsal longitudinal anastomotic vessel (DLAV) and intersegmental vessels (Fig. 1E). These defects were even more pronounced after injection of 2 ng MOegf.

Taken together, our results clearly show that inhibition of the Egf pathway, by genetic down-regulation of Egf expression, leads to combined defects in cartilage development, blood vessel function in the trunk and *mbp* expression.

Developmental defects caused by inhibition of EGFR function

Having established several developmental defects resulting from inhibition of Egf expression, we decided to investigate the effects caused by tyrphostins known to inhibit Egf signaling, such as AG-1478, AG-18, AG-213 (Szende et al., 1995), AG-490 and AG-825.

Lethality and morphological defects caused by EGFR inhibitors. As a first step in the characterization of their biological properties, the survival of zebrafish larvae exposed to different concentrations of the selected EGFR inhibitors was determined. Inhibitor treatments were initiated at 4 hpf during 4 days and survival rates were determined. LC50 and LC10 concentrations were calculated at 96 hpf (Table 1). While no effect on survival was observed at any time point following exposure to 1% DMSO, the highest concentration of solvent used in these experiments, AG-1478 was found to be lethal at 4 dpf with LC50 = 9.5 μM and LC10 = 7.7 μM (Fig. 3A, Table 1). AG-490, AG-825 and AG-18 exposure proved to be lethal with respectively calculated LC50 = 60, 11 and 77 μM, while AG-213 caused no lethality at the highest concentration tested (Fig. 3B–E, Table 1).

We also determined the morphological defects present in the surviving larvae at 4 dpf. The results of these observations and the proportions of the larvae presenting the various defects are summarized in Table 2. EC50 concentrations were determined for occurrence of any morphological defect and the teratogenic index (TI = LC50/EC50) was calculated (Fig. 3A–E, Table 3). AG-1478 exposure induces edema (from 2 ± 2% at 2.5 μM to 97 ± 3% at 10 μM) and tail curvatures (from 4 ± 4% at 7.5 μM to 64 ± 8% at 10 μM) at 4 dpf with EC50 and EC10 of, respectively 7.8 and 7 μM (Table 2). AG-18 at 10 μM exposure induced edema and growth retardation (respectively 12 ± 10 and 40 ± 20%

Table 1
Molecules tested and their effects on lethality. The table shows the name, chemical structure and molecular weight of the different inhibitors tested here. The results of the lethality tests after exposure from 4 hpf to 4 dpf are given as LC50 and LC10 and their known pharmacological effects are indicated.

		MW	LC50	LC10	
AG-1478	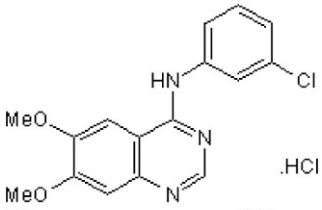	352.2	9.5 μM	7.7 μM	EGFR kinase inhibitor
AG-18	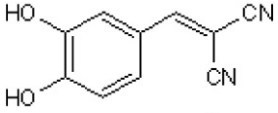	186.2	77 μM	40 μM	EGFR/PDGFR inhibitor
AG-213	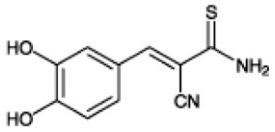	220.2	>100 μM	>100 μM	EGFR receptor kinase inhibitor
AG-490	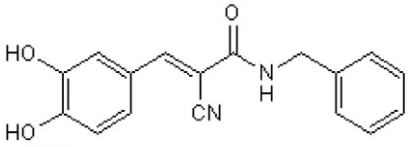	294.3	60 μM	49 μM	EGF receptor tyrosine kinase inhibitor
AG-825	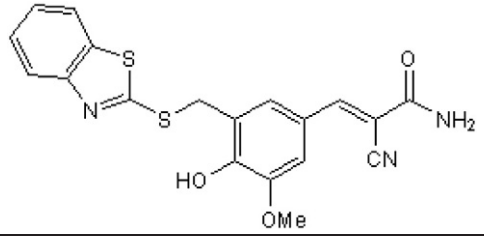	397.5	11 μM	4.4 μM	ErbB2 inhibitor

of observed larvae). At 25 μM, AG-18 caused additional tail curvature in 10 ± 7% of the exposed larvae, while at 100 μM all observed larvae presented morphological defects (Table 2). EC50 was calculated to be 53 μM. AG-213 exposure did not cause significant morphological defects at the different tested concentrations, its EC50 is higher than 100 μM. Zebrafish larvae exposed to AG-490 10 μM presented growth retardation and tail curvature in 42 ± 2% of observed larvae, while additional edema and shorter tails were observed at higher concentrations. EC50 for AG-490 was found to be 20 μM. AG-825 caused growth retardation in all larvae, even at the lowest tested concentration (5 μM), while 55 ± 30% of those larvae also presented edema. At higher concentrations (10 and 25 μM), edema was observed in most larvae (respectively 90 ± 14% and 100%) in addition to growth retardation and a shorter tail reported in all larvae. EC50 was lower than 5 μM for AG-825.

The teratogenic index (TI) was also calculated as LC50/EC50 (Table 3). While the effects observed with AG-18 (TI = 1.43) and AG-1478 (TI = 1.22) may be closely related to their lethality, AG-825 (TI = 2.37) and AG-490 (TI = 3.04) clearly revealed their teratogenicity (TI ≫ 1).

Egfr inhibitors cause developmental defects in head cartilage. To investigate the defects in skeletal development associated with Egfr inhibition in zebrafish, we analyzed head cartilage formation at 4 dpf by alcian blue staining. The resulting cartilage profiles were classified in the four types (Fig. 2) and cartilage EC50 (cE50) was calculated based on the presence of any cartilage defect (type II, III or IV) (Fig. 3F-J, Table S1) as described above.

Exposure to AG-1478 lead to concentration-dependant cartilage malformations, ranging from 37 ± 30% type II cartilage at 1 μM to 93 ± 4 at 2.5 μM. More severely altered patterns were observed at 5 μM (14 ± 13 type III), 7.5 μM (25 ± 31 type III and 6 ± 8 type IV) and 10 μM (88 ± 12 type III and 12 ± 12 type IV (Fig. 3F, Table S1). cEC50 was found to be 1.12 μM for AG-1478 (Fig. 3F, Tables S1 and 4). To assess the specificity of the cartilage defects generated by the inhibitor, a "cartilage defect index" (CI) was calculated (CI = LC50/cEC50) similar to the well-known teratogenic index. The CI for AG-1478 exposure was CI = 8.50 (Table 4), indicating that inhibition of the Egf pathway leads to specific defects in cartilage development (CI ≫ 1).

When exposed to AG-18, the larvae presented a significantly altered cartilage only at 100 μM exposure, characterized by type III (50 ± 17%) and type IV (50 ± 17%) patterns (Fig. 3G; Table S1). AG-213 caused a weak, but dose-dependant increase of abnormal cartilage formation (10 ± 5% type II cartilage at 100 μM (Fig. 3H and Table S1). AG-490 exposure led to type II (33 ± 27%) and type III (20 ± 7%) cartilage defects at 50 μM, while 7 ± 10% of exposed larvae exhibited a severe alteration (type IV) (Fig. 3I; Table S1). At 5 μM, AG-825 exposure led only to 34 ± 4% of weakly affected (type II) cartilage profiles, a 10 μM exposure caused type II (28 ± 24%), type III (39 ± 18%) and type IV (33 ± 9%) patterns (Fig. 3J, Table S1).

While cEC50 for AG-213 was found to be higher than 100 μM, cEC50 of AG-18, AG-490, AG-825 were found to be respectively 60 μM, 45 μM and 5 μM (Table 4). cEC50 were found to be close to LC50 for AG-18 (CI = 1.3) and AG-490 (CI = 1.3), whereas AG-825 (CI = 2.2) presents a specific effect on cartilage development (Table 4).

Effects of Egfr inhibitors on myelin formation. Previously, AG-1478 exposure was shown to prevent expression of the myelin-specific protein Mbp (myelin basic protein) in zebrafish larvae (Lyons et al., 2005). To

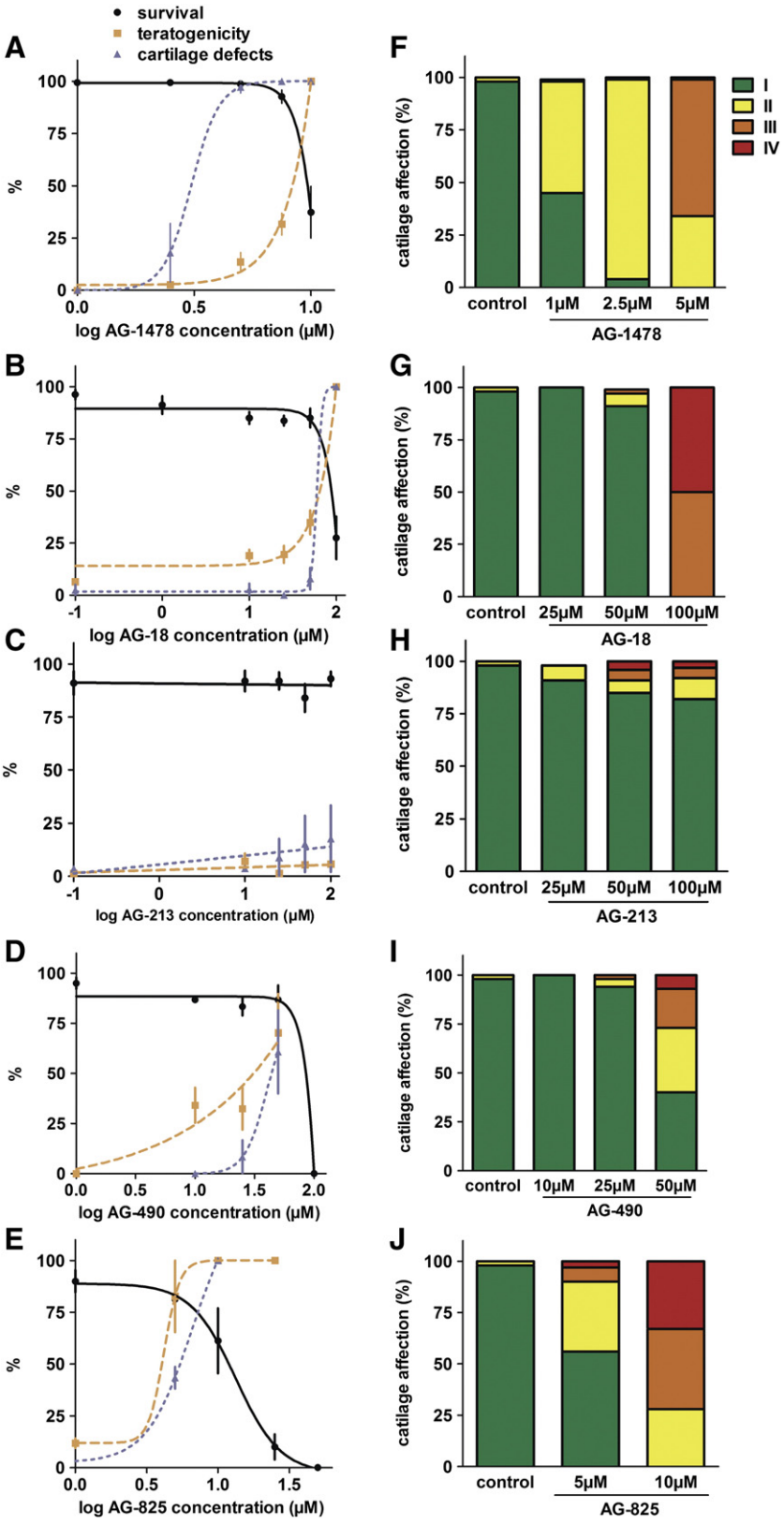

Fig. 3. Survival, teratogenicity and cartilage defects upon exposure to EGF pathway inhibitors. (A–E) Fraction of surviving larvae (black line); larvae presenting any morphological defect (orange dotted line) or any cartilage defect (purple dotted line) at 4 dpf upon daily exposure to different concentrations of AG-1478 (A) AG-18 (B), AG-213 (C), AG-490 (D) or AG-825(E) with their corresponding SD. (F–J) proportions of head cartilage patterns observed on larvae exposed to AG-1478 (F) AG-18 (G), AG-213 (H), AG-490 (I) and AG-825(J) at the indicated concentrations from 4 hpf to 4 dpf. (I. no observable defect; II. shortened Meckel's cartilage; III. shortened Meckel's cartilage associated with attenuated or absence of ceratobranchials; IV. without any cartilage formation.). (For interpretation of the references to color in this figure legend, the reader is referred to the web version of this article.)

Table 2
Inhibitors and associated morphological defects.The table shows the proportions of larvae presenting the different morphological defects (edema, growth retardation, curved tail, short tail and hemorrhages) upon exposure to the different drugs at the indicated concentrations from 4 hpf to 4 dpf.

	Concentration (μM)	Edema	Growth retardation	Curved tail	Short tail	Hemorrhages
AG-1478	1	–	–	–	–	–
	2.5	2 ± 2	–	–	–	2 ± 2
	5.0	5 ± 5	–	0.7 ± 1	–	9 ± 5
	7.5	15 ± 14	–	4 ± 4	0.7 ± 1	14 ± 12
	10	97 ± 3	4 ± 4	64 ± 8	4 ± 4	5 ± 2
AG-18	10	12 ± 10	40 ± 20	–	–	–
	25	18 ± 10	14 ± 13	10 ± 7	–	–
	50	12 ± 6	23 ± 17	20 ± 16	–	–
	100	100 ± 0	100 ± 0	100 ± 0	100 ± 0	–
AG-213	10	–	–	–	4 ± 6	–
	25	–	–	–	–	–
	50	5 ± 3	–	–	4 ± 3	–
	100	6 ± 8	5.7 ± 0.2	2 ± 2	–	–
AG-490	10	–	42 ± 2	42 ± 2	–	–
	25	11 ± 11	34 ± 6	3 ± 3	6 ± 6	–
	50	83 ± 1	83 ± 1	83 ± 1	92 ± 7	–
AG-825	5	55 ± 30	100 ± 0	–	–	–
	10	90 ± 14	100 ± 0	–	100 ± 0	–
	25	100 ± 0	100 ± 0	–	100 ± 0	–

confirm and extend this observation, we analyzed *mbp* expression in 4 dpf larvae by RT-qPCR quantification of whole body mRNA levels. AG-1478 inhibited *mbp* expression in larvae exposed to 0.5, 1.1 and 1.5 μM with respectively 2.2-, 3.3- and 3.6-fold decreases (Fig. 4A). By whole-mount *in situ* hybridization, we observed that AG-1478 treatment resulted in a drastic, dose-dependant decrease of *mbp* expression, leaving only a weak expression in the hindbrain at 1.5 μM (Fig. 4B).

The expression of *mbp* was also analyzed following exposure to the other tyrphostins at concentrations corresponding to the previously determined cEC50 values. While no alteration of *mbp* expression could be associated to AG-213 exposure, a weak decrease (1.24 fold) was observed in larvae exposed to AG-825 by RT-qPCR. AG-18 caused a stronger decrease (1.6 fold) in *mbp* expression, while AG-490 treatment resulted in a dramatic (5.7 fold) inhibition (Fig. 5A). WISH analysis confirmed the impact of AG-490 exposure on *mbp* expression, especially in the lateral line (Fig. 5B).

Tyrphostins inhibit blood flow in intersomitic vessels of the trunk. Previously, 10 μM AG-1478 treatment was shown to impair intersomitic blood vessel development (Tran et al., 2007). To confirm and further characterize those results, micro-angiography was performed on tyrphostin-exposed larvae as described above. In AG-1478 treated larvae, blood circulation was interrupted in the most posterior regions and in patches of the cardinal vein and the intersomitic vessels (Fig. 6). These defects were more intense at higher inhibitor concentrations, although the formation of the various blood vessels seemed only slightly affected at the concentrations used here. While AG-213 exposed larvae appeared unaltered, AG-18 exposure led to an absence of circulation in the caudal tip, especially in the dorsal longitudinal anastomotic vessel (DLAV) and a reduced circulation in the caudal vein (CV) (Fig. 6). The same effect on CV was obtained upon AG-490 exposure associated with the absence of circulation in some intersegmental vessels (Se). AG-825 induced a strong circulation defect characterized by a complete absence in the caudal tip and absence of blood flow in intersegmental vessels, the posterior part of DLAV and also in the caudal vein.

Thus, we observe clear developmental defects in cartilage, myelin and blood circulation upon treatment with the Egf inhibitors at sublethal concentrations.

Discussion

In this study, we decided to define several developmental defects resulting from impairment of the Egf signaling pathway by comparing the effects due to direct, genetic knock-down of Egf expression with those observed upon treatment with known inhibitors of its signaling pathway.

When Egf expression was decreased by microinjection of specific antisense morpholinos to block correct splicing of the *egf* mRNA, no major morphological defects, such as edema or necrosis were observed even at the highest concentration of MOegf tested and lethality was very low. In contrast, we observed a decrease of *mpb* expression by *in situ* hybridization and we further confirmed *mbp* mRNA depletion by qRT-PCR analysis already at the smallest amount (0.5 ng) of MOegf injected. This observation is consistent with the previously observed decrease of *mbp* expression in *erbb2* and *erbb3* mutants (Lyons et al., 2005), indicating that these receptors are required for transmission of the Egf signal in these cells. Similarly, we observed a clear interruption of blood circulation in the trunk vessels by microangiography at this concentration, reminiscent of the previously observed effect on angiogenesis of the

Table 3
Molecules tested and their effects on morphology.The effective concentrations (EC50, EC10) to cause any morphological defect are given for exposure to the indicated inhibitors from 4 hpf to 4 dpf with a daily renewal, as well as the teratogenic index (TI) and the morphological defects that were observed for each drug.

	EC50	EC10	TI	Morphological defects
AG-1478	**7.8 μM**	**7.0 μM**	**1.22**	Edema Curved tail Hemorrhages
AG-18	**53 μM**	**50.5 μM**	**1.43**	Edema Growth retardation Short curved tail
AG-213	>**100 μM**	>**100 μM**	/	Edema Growth retardation Curved tail
AG-490	**19.6 μM**	**3.8 μM**	**3.04**	Edema Growth retardation Short curved tail
AG-825	**4.7 μM**	**3.8 μM**	**2.37**	Edema Growth retardation Short tail

Table 4
Molecules tested and their effects on cartilage.The effective concentrations (cEC50, cEC10) to cause any cartilage defect are given for exposure to the indicated inhibitors from 4 hpf to 4 dpf with a daily renewal, as well as the cartilage defect index (CI) for each drug.

	cEC50	cEC10	CI
AG-1478	1.1 μM	0.68 μM	8.50
AG-18	60 μM	51 μM	1.28
AG-213	>100 μM	ND	–
AG-490	45 μM	26 μM	1.33
AG-825	5.0 μM	4.3 μM	2.23

inhibitor AG-1478 (Tran et al., 2007). In addition, we describe for the first time that Egf signaling is required for the formation of head cartilage in 96 hpf zebrafish embryos. *egf* knock-down leads to dose-dependent defects in cartilage formation, consistent with the previously described involvement of the Egf pathway in cartilage and bone formation in rats (Zhang et al., 2011), mutant mice (Miettinen et al., 1999; Sibilia et al., 2003; Wang et al., 2004), cartilage explants (Shum et al., 1993) and cell lines (Fisher et al., 2007; Takeda et al., 2010). Taken together, we describe three developmental defects in 96 hpf zebrafish larvae that are observed upon knock-down of Egf expression without any evidence of unspecific teratogenic effects or lethality: impaired cartilage formation, decrease of *mbp* expression and partial interruption of blood flow in the trunk.

Having defined these specific indicators for Egf signal depletion, we determined the biological effects of several tyrphostins known to inhibit Egfr function. Concerning lethality and morphological defects, AG-490 and AG-825 are clearly teratogenic (TI of, respectively 3 and 2.37), while AG-213 did not cause any significant effect at the highest concentration tested (100 μM). AG-18 was only weakly teratogenic (TI = 1.43), similar to AG-1478 (TI = 1.22), albeit at a much higher concentration (EC50 = 53 μM). The consequences of tyrphostin exposure on cartilage formation were then determined and cEC50 was calculated for all tested compounds. In contrast to the effect of AG-1478 at clearly non-teratogenic concentrations, AG-18, AG-490 and AG-825 were found to impair cartilage development after exposure at concentrations close to teratogenic conditions.

To be able to compare the effects on different processes for each compound, we used the response on cartilage formation as a reference. We chose the corresponding cEC50 concentration to determine the extent of impairment of *mbp* expression and blood flow in the trunk. Consistent with previous data (Lyons et al., 2005), AG-1478 treatment caused a reduction of *mbp* expression by 70% at 1.1 μM (cEC50) and by 55% at 0.5 μM (below cEC10). AG-18, AG-490 and, to a lesser extent, AG-825 exposure lead to a significant decrease of myelination in zebrafish larvae at their respective cEC50. Microangiography revealed circulatory defects upon AG-1478, AG-18, AG-490 or AG-825 treatment, while no alteration of the vessel pattern could be observed. Our approach to test in parallel the effects of various inhibitors on different processes allows a direct comparison of their dose-response relationship and thus their link to the targeted pathway. The fact that the cartilage, blood circulation and *mbp* expression effects are observed at the same, largely sub lethal concentrations (0.5–1.5 μM) of the inhibitor AG-1478 further supports their specificity for the Egf pathway. In contrast, morphological malformations such as edema, hemorrhage or curved tail were observed at about 10-fold higher concentrations of AG-1478, but were not observed even at the highest concentrations of MOegf tested. Their occurrence at close to lethal concentrations (TI close to 1) argues in favor of an unspecific effect, however they could also be caused by inhibition of receptor activation by another Egfr ligand (Tgfα, HBEgf). The same high concentration of AG-1478 (10 μM) was previously shown to impair blood vessel formation (Tran et al., 2007), while knock-down of Egf expression did not cause these defects, indicating yet another unspecific or off-target effect.

A comparison of the effects on developmental impairment observed for the different treatments is summarized in Table 5. AG-213 seems to be inactive and will not further be discussed. The other inhibitors affect cartilage formation, *mbp* expression and blood circulation at varying degrees, indicating that they act on the Egf pathway. AG-1478 appears as the most specific, as expected, as it exerts its specific effects at concentrations much lower than its LC50 or EC50 (cEC50 = 1.1 μM and 0.3-fold expression of *mbp* at this concentration). AG-18, AG-490 and AG-825 all present a cEC50 for cartilage defects below their LC50, but close to or higher than their EC50, indicating that they cause additional, morphological defects. However, despite these morphological defects, we could readily observe the three indicators for impairment of the Egf pathway at this concentration. AG-490 caused a decrease of *mbp* expression by 80% relative to control, close to the 70% observed upon AG-1478 treatment. AG-18 and AG-825 caused a weaker, but significant reduction of *mbp* expression by, respectively 40 and 20%. Similarly, all inhibitors (except AG-213) were shown to affect trunk blood circulation at their corresponding cEC50. Taken together, these observations lead to the conclusion that AG-1478 is a specific Egf inhibitor at concentrations with only little side effects, AG-490 is able

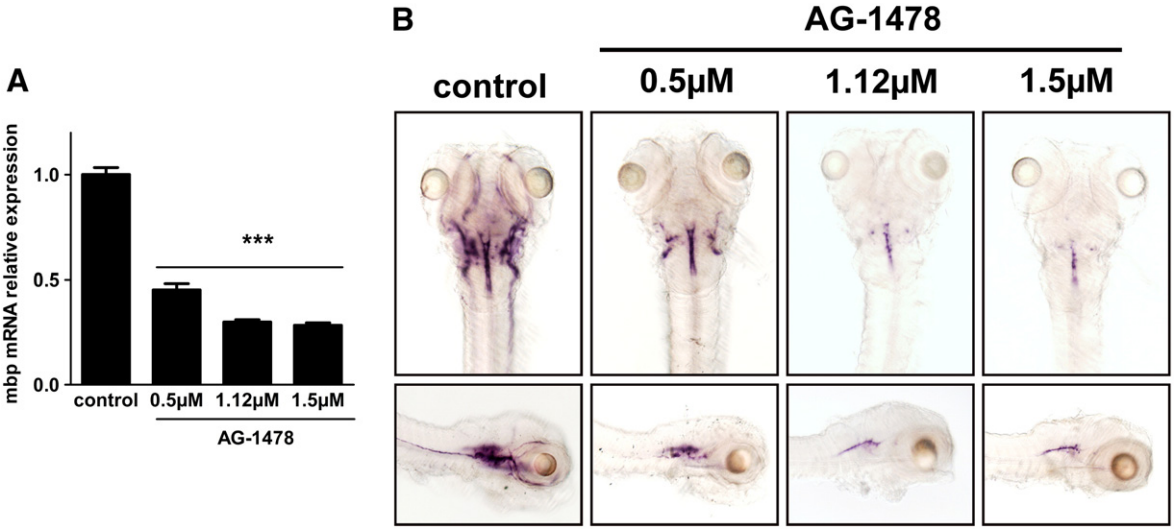

Fig. 4. Myelin basic protein expression upon AG-1478 exposure in 96 hpf zebrafish embryos. Myelin basic protein gene expression analysis by qPCR (A) and whole mount *in situ* hybridization (B) upon exposure to AG-1478 at the indicated concentrations from 4 hpf to 4 dpf. The columns represent the mean ± SD of three samples; *** statistically different from control ($P < 0.005$).

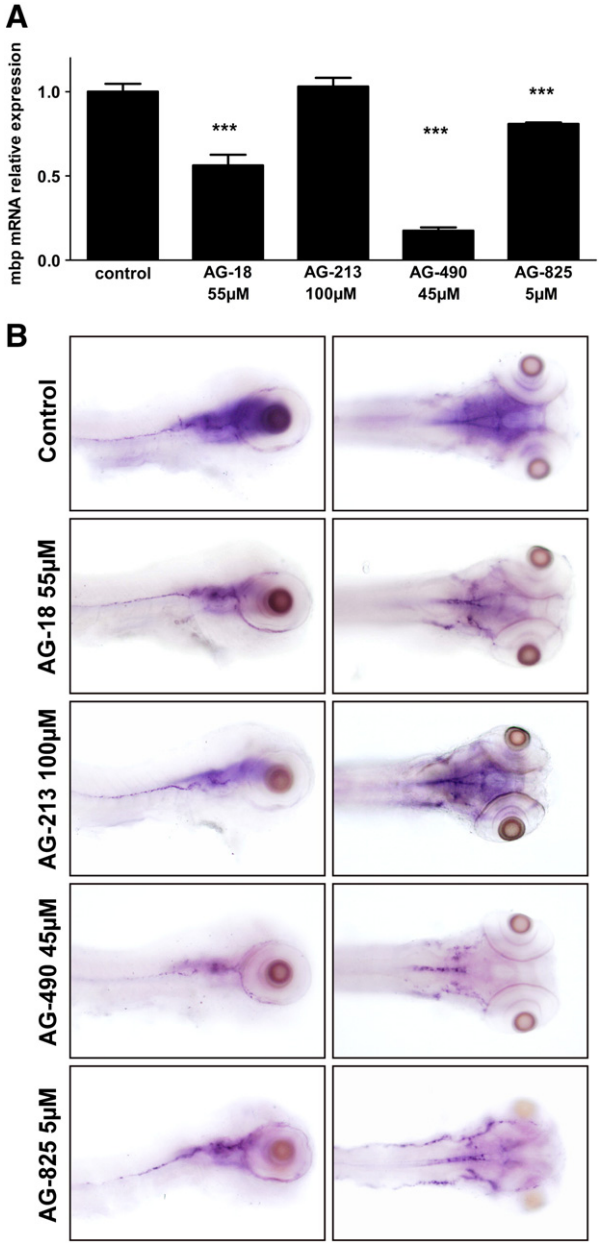

Fig. 5. Myelin basic protein expression upon AG-18, AG-213, AG-490 or AG-825 exposure in 96 hpf zebrafish embryos. Myelin basic protein gene expression analysis by qPCR (A) and whole mount *in situ* hybridization (B) upon exposure to EGFR inhibitors at cEC50 concentrations from 4 hpf to 4 dpf. The columns represent the mean ± SD of three samples; *** statistically different from control ($P < 0.005$).

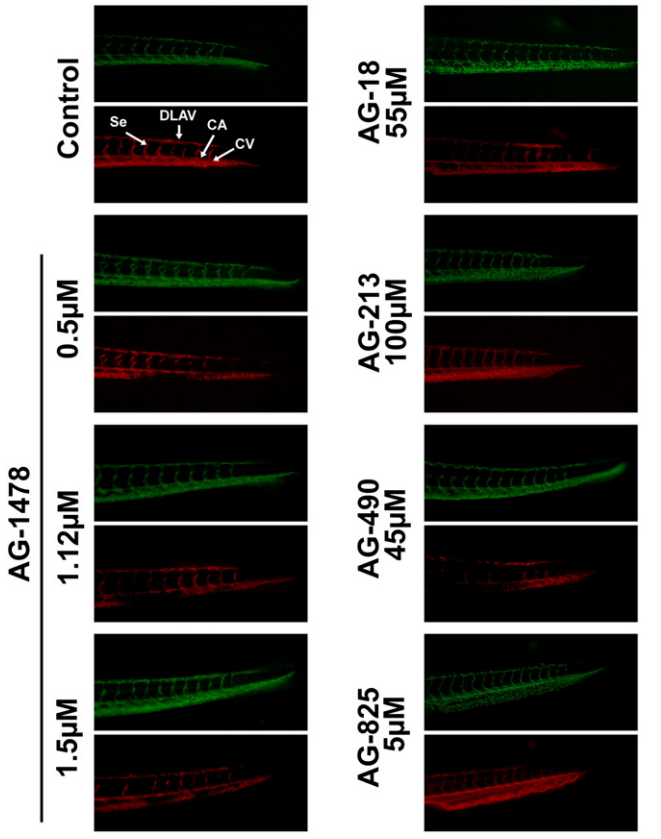

Fig. 6. Effects of EGF pathway inhibitors on trunk vessel formation and function. Microangiography in transgenic fli-GFP embryos exposed to solvent or to EGFR inhibitors at cEC50 concentrations from 4 hpf to 4 dpf. (A: aorta; CV: Cardinal vein; DLAV: Dorsal longitudinal anastomotic vessel and Se: intersegmental vessels.).

to inhibit Egf signaling but at concentrations where it causes serious side effects, while AG-18 and AG-825 are poorly specific inhibitors.

Our observation that Egf signaling is specifically involved in cartilage formation, *mbp* expression and blood circulation indicates that the maintenance, restoration or even pharmacological activation of this pathway might represent a promising target for treatment of disorders affecting one of these phenomena.

In addition to the three developmental defects associated to disruption of Egf signaling, other morphological effects were observed upon treatment by the different inhibitors. Although these effects might be considered as non-specific, some interesting differences are however apparent. AG-1478 caused growth retardation and shortened tails only very marginally (4% at 10 μM), similar to Egf knock-down, in contrast to AG-18, AG-490 or AG-825 (Table 2). These effects are probably due to inhibition of some other signaling pathway, erbB2, erbB3, erbB4 or Pdgf (Bilder et al., 1991; Osherov et al., 1993; Rendu et al., 1992). AG-1478 also had a low, but significant incidence of hemorrhages that was not observed with any other tyrphostin or even the highest concentration of MOegf, suggesting yet another off-target effect. Chemically, AG-1478 is related to other quinazolin-derived compounds (Table 1) that present a good specificity for egfr1, such as erlotinib or gefitinib, but were shown to also inhibit ErbB3 and ErbB4 phosphorylation on cells cultured *in vitro* (Carrasco-Garcia et al., 2011). The other compounds tested here are benzenemalononitrile derivatives (Levitzki and Gazit, 1995) that also inhibit Pdgf signaling to various degrees (Bilder et al., 1991). Compounds that couple a hydroxy-benzyl group to the malononitrile group through a double bond such as AG-18 (Table 1) present an additional activity as mitochondrial uncouplers (Soltoff, 2004). Substitution of one nitrile group in AG-490 leads (Table 1) to additional inhibition of Jak-2 (Meydan et al., 1996) and Jak2a in zebrafish (Ma et al., 2007), while multiple substitutions as in AG-825 lead to specific inhibition of egfr2. Further experiments will be required to attribute the observed off-target effects to one or several alternative pathways.

In conclusion, by combining genetic inactivation and specific inhibition of the pathway, we were able to define developmental defects that can serve as indicators for inactivation of Egf signaling: impairment of cartilage formation, decrease of *mbp* expression and perturbation of trunk blood circulation. Genetic inactivation of Egf expression resulted in the lowest occurrence of non-specific effects, while chemical inhibitors of Egfr function caused these indicator defects with various specificities. In future drug screening efforts, instead of rejecting a compound because of excessive teratogenicity and/or lethality, observation of the three independent developmental defects specific for Egf inactivation

Table 5
Developmental defects due to impairment of Egf signaling.Summary table showing the lethal and effective concentrations for each tested inhibitor as well as their effect, in comparison to MO concentrations, on *mbp* expression and blood circulation.

	LC50 μM	EC50 μM	cEC50 μM	Mbp fold inhib	circulation
MOegf 0.5 ng				0.5	+
MOegf 1 ng				0.4	+
MOegf 2 ng				0.2	+
AG-1478	9.5	7.8	1.1	0.3	+
AG-18	77	53.5	60	0.6	+
AG-213	>100	>100	>100	1.0	−
AG-490	60	19.6	45	0.2	+
AG-825	11	4.7	5.0	0.8	+

will justify further investigations into increasing the specificity of that compound. On the other end, knowledge of the specific developmental defects will also allow evaluating off-target effects in a whole animal setting of compounds considered as highly specific by *in vitro* tests. In addition, observation of specific off-target effects might lead to new applications, if a possible target causing this defect is known. Other target-oriented drug screening programs will benefit from comparison of drug effects on zebrafish development to those caused by genetic inactivation of the target molecule.

Supplementary data to this article can be found online at http://dx.doi.org/10.1016/j.taap.2013.11.006.

Conflict of interest statement

All authors declare that they have no conflicts of interest concerning this work.

Acknowledgments

This work was supported by the Walloon Region (FEDER. GIGA2 Bioindustry support), the European Interreg Program Alma-in-silico (AIS) and the Fonds National de la Recherche Scientifique (F.N.R.S.). M.M. is a “Chercheur Qualifié du F.N.R.S.” We wish to thank the GIGA-R zebrafish facility for providing zebrafish adults and fertilized eggs and the GIGA-R GenoTranscriptomics platform for DNA sequencing and RNA quality control. This is the AFFISH (Applied and Fish Research Center) publication no 17.

References

Aguirre, A., Dupree, J.L., Mangin, J.M., Gallo, V., 2007. A functional role for EGFR signaling in myelination and remyelination. Nat. Neurosci. 10, 990–1002.
Asakura, M., Kitakaze, M., Takashima, S., Liao, Y., Ishikura, F., Yoshinaka, T., Ohmoto, H., Node, K., Yoshino, K., Ishiguro, H., Asanuma, H., Sanada, S., Matsumura, Y., Takeda, H., Beppu, S., Tada, M., Hori, M., Higashiyama, S., 2002. Cardiac hypertrophy is inhibited by antagonism of ADAM12 processing of HB-EGF: metalloproteinase inhibitors as a new therapy. Nat. Med. 8, 35–40.
Barker, A.J., Gibson, K.H., Grundy, W., Godfrey, A.A., Barlow, J.J., Healy, M.P., Woodburn, J.R., Ashton, S.E., Curry, B.J., Scarlett, L., Henthorn, L., Richards, L., 2001. Studies leading to the identification of ZD1839 (IRESSA): an orally active, selective epidermal growth factor receptor tyrosine kinase inhibitor targeted to the treatment of cancer. Bioorg. Med. Chem. Lett. 11, 1911–1914.
Bianco, R., Gelardi, T., Damiano, V., Ciardiello, F., Tortora, G., 2007. Rational bases for the development of EGFR inhibitors for cancer treatment. Int. J. Biochem. Cell Biol. 39, 1416–1431.
Bilder, G.E., Krawiec, J.A., McVety, K., Gazit, A., Gilon, C., Lyall, R., Zilberstein, A., Levitzki, A., Perrone, M.H., Schreiber, A.B., 1991. Tyrphostins inhibit PDGF-induced DNA synthesis and associated early events in smooth muscle cells. Am. J. Physiol. 260, C721–C730.
Blume-Jensen, P., Hunter, T., 2001. Oncogenic kinase signalling. Nature 411, 355–365.
Bulic, B., Ness, J., Hahn, S., Rennhack, A., Jumpertz, T., Weggen, S., 2011. chemical biology, molecular mechanism and clinical perspective of gamma-secretase modulators in Alzheimer's disease. Curr. Neuropharmacol. 9, 598–622.
Caja, L., Sancho, P., Bertran, E., Ortiz, C., Campbell, J.S., Fausto, N., Fabregat, I., 2011. The tyrphostin AG1478 inhibits proliferation and induces death of liver tumor cells through EGF receptor-dependent and independent mechanisms. Biochem. Pharmacol. 82, 1583–1592.
Carrasco-Garcia, E., Saceda, M., Grasso, S., Rocamora-Reverte, L., Conde, M., Gomez-Martinez, A., Garcia-Morales, P., Ferragut, J.A., Martinez-Lacaci, I., 2011. Small tyrosine kinase inhibitors interrupt EGFR signaling by interacting with erbB3 and erbB4 in glioblastoma cell lines. Exp. Cell Res. 317, 1476–1489.
Chang, C., Sternberg, P.W., 1999. *C. elegans* vulval development as a model system to study the cancer biology of EGFR signaling. Cancer Metastasis Rev. 18, 203–213.
Crone, S.A., Zhao, Y.Y., Fan, L., Gu, Y., Minamisawa, S., Liu, Y., Peterson, K.L., Chen, J., Kahn, R., Condorelli, G., Ross Jr., J., Chien, K.R., Lee, K.F., 2002. ErbB2 is essential in the prevention of dilated cardiomyopathy. Nat. Med. 8, 459–465.
Dalcq, J., Pasque, V., Ghaye, A., Larbuisson, A., Motte, P., Martial, J.A., Muller, M., 2012. Runx3, Egr1 and Sox9b form a regulatory cascade required to modulate BMP-signaling during cranial cartilage development in zebrafish. PLoS One 7, e50140.
Dienstmann, R., Brana, I., Rodon, J., Tabernero, J., 2011. Toxicity as a biomarker of efficacy of molecular targeted therapies: focus on EGFR and VEGF inhibiting anticancer drugs. Oncologist 16, 1729–1740.
Eccles, S.A., 2011. The epidermal growth factor receptor/Erb-B/HER family in normal and malignant breast biology. Int. J. Dev. Biol. 55, 685–696.
Fisher, M.C., Clinton, G.M., Maihle, N.J., Dealy, C.N., 2007. Requirement for ErbB2/ErbB signaling in developing cartilage and bone. Dev. Growth Differ. 49, 503–513.
Friedrichs, F., Zugck, C., Rauch, G.J., Ivandic, B., Weichenhan, D., Muller-Bardorff, M., Meder, B., El Mokhtari, N.E., Regitz-Zagrosek, V., Hetzer, R., Schafer, A., Schreiber, S., Chen, J., Neuhaus, I., Ji, R., Siemers, N.O., Frey, N., Rottbauer, W., Katus, H.A., Stoll, M., 2009. HBEGF, SRA1, and IK: three cosegregating genes as determinants of cardiomyopathy. Genome Res. 19, 395–403.
Gibbs, J.B., 2000. Mechanism-based target identification and drug discovery in cancer research. Science 287, 1969–1973.
Goishi, K., Lee, P., Davidson, A.J., Nishi, E., Zon, L.I., Klagsbrun, M., 2003. Inhibition of zebrafish epidermal growth factor receptor activity results in cardiovascular defects. Mech. Dev. 120, 811–822.
Harari, P.M., Allen, G.W., Bonner, J.A., 2007. Biology of interactions: antiepidermal growth factor receptor agents. J. Clin. Oncol. 25, 4057–4065.
Hardy, K.M., Booth, B.W., Hendrix, M.J., Salomon, D.S., Strizzi, L., 2010. ErbB/EGF signaling and EMT in mammary development and breast cancer. J. Mammary Gland Biol. Neoplasia 15, 191–199.
Hauptmann, G., Gerster, T., 2000. Multicolor whole-mount in situ hybridization. Methods Mol. Biol. 137, 139–148.
Holbro, T., Hynes, N.E., 2004. ErbB receptors: directing key signaling networks throughout life. Annu. Rev. Pharmacol. Toxicol. 44, 195–217.
Iwamoto, R., Mekada, E., 2006. ErbB and HB-EGF signaling in heart development and function. Cell Struct. Funct. 31, 1–14.
Jost, M., Kari, C., Rodeck, U., 2000. The EGF receptor — an essential regulator of multiple epidermal functions. Eur. J. Dermatol. 10, 505–510.
Kang, N., Zhang, J.H., Qiu, F., Tashiro, S., Onodera, S., Ikejima, T., 2010. Inhibition of EGFR signaling augments oridonin-induced apoptosis in human laryngeal cancer cells via enhancing oxidative stress coincident with activation of both the intrinsic and extrinsic apoptotic pathways. Cancer Lett. 294, 147–158.
Kimmel, C.B., Ballard, W.W., Kimmel, S.R., Ullmann, B., Schilling, T.F., 1995. Stages of embryonic development of the zebrafish. Dev. Dyn. 203, 253–310.
Laisney, J.A., Braasch, I., Walter, R.B., Meierjohann, S., Schartl, M., 2010. Lineage-specific co-evolution of the Egf receptor/ligand signaling system. BMC Evol. Biol. 10, 27.
Langer, C.J., 2007. Mind your elders: therapeutic implications of epidermal growth factor receptor inhibition in older patients with advanced non-small-cell lung cancer. J. Clin. Oncol. 25, 751–753.
Levitzki, A., Gazit, A., 1995. Tyrosine kinase inhibition: an approach to drug development. Science 267, 1782–1788.
Li, T., Perez-Soler, R., 2009. Skin toxicities associated with epidermal growth factor receptor inhibitors. Target. Oncol. 4, 107–119.
Lu, X., Kang, Y., 2010. Epidermal growth factor signalling and bone metastasis. Br. J. Cancer 102, 457–461.
Luetteke, N.C., Phillips, H.K., Qiu, T.H., Copeland, N.G., Earp, H.S., Jenkins, N.A., Lee, D.C., 1994. The mouse waved-2 phenotype results from a point mutation in the EGF receptor tyrosine kinase. Genes Dev. 8, 399–413.
Lyons, D.A., Pogoda, H.M., Voas, M.G., Woods, I.G., Diamond, B., Nix, R., Arana, N., Jacobs, J., Talbot, W.S., 2005. erbb3 and erbb2 are essential for schwann cell migration and myelination in zebrafish. Curr. Biol. 15, 513–524.
Ma, A.C., Ward, A.C., Liang, R., Leung, A.Y., 2007. The role of jak2a in zebrafish hematopoiesis. Blood 110, 1824–1830.
Maccari, R., Paoli, P., Ottana, R., Jacomelli, M., Ciurleo, R., Manao, G., Steindl, T., Langer, T., Vigorita, M.G., Camici, G., 2007. 5-Arylidene-2,4-thiazolidinediones as inhibitors of protein tyrosine phosphatases. Bioorg. Med. Chem. 15, 5137–5149.
Meydan, N., Grunberger, T., Dadi, H., Shahar, M., Arpaia, E., Lapidot, Z., Leeder, J.S., Freedman, M., Cohen, A., Gazit, A., Levitzki, A., Roifman, C.M., 1996. Inhibition of acute lymphoblastic leukaemia by a Jak-2 inhibitor. Nature 379, 645–648.
Miettinen, P.J., Chin, J.R., Shum, L., Slavkin, H.C., Shuler, C.F., Derynck, R., Werb, Z., 1999. Epidermal growth factor receptor function is necessary for normal craniofacial development and palate closure. Nat. Genet. 22, 69–73.
Morizot, D.C., McEntire, B.B., Della Coletta, L., Kazianis, S., Schartl, M., Nairn, R.S., 1998. Mapping of tyrosine kinase gene family members in a *Xiphophorus* melanoma model. Mol. Carcinog. 22, 150–157.
Olayioye, M.A., Neve, R.M., Lane, H.A., Hynes, N.E., 2000. The ErbB signaling network: receptor heterodimerization in development and cancer. EMBO J. 19, 3159–3167.
Osherov, N., Gazit, A., Gilon, C., Levitzki, A., 1993. Selective inhibition of the epidermal growth factor and HER2/neu receptors by tyrphostins. J. Biol. Chem. 268, 11134–11142.

Pan, S.N., Ma, H.M., Su, Z., Zhang, C.X., Zhu, S.Y., Du, M.L., 2011. Epidermal growth factor receptor signalling mediates growth hormone-induced growth of chondrocytes from sex hormone-inhibited adolescent rats. Clin. Exp. Pharmacol. Physiol. 38, 534–542.
Pang, Y., Ge, W., 2002. Epidermal growth factor and TGFalpha promote zebrafish oocyte maturation in vitro: potential role of the ovarian activin regulatory system. Endocrinology 143, 47–54.
Pastore, S., Mascia, F., Mariani, V., Girolomoni, G., 2008. The epidermal growth factor receptor system in skin repair and inflammation. J. Invest. Dermatol. 128, 1365–1374.
Pfaffl, M.W., 2001. A new mathematical model for relative quantification in real-time RT-PCR. Nucleic Acids Res. 29, 2002–2007.
Rendu, F., Eldor, A., Grelac, F., Bachelot, C., Gazit, A., Gilon, C., Levy-Toledano, S., Levitzki, A., 1992. Inhibition of platelet activation by tyrosine kinase inhibitors. Biochem. Pharmacol. 44, 881–888.
Saito, K., Horiuchi, K., Kimura, T., Mizuno, S., Yoda, M., Morioka, H., Akiyama, H., Threadgill, D., Okada, Y., Toyama, Y., Sato, K., 2013. Conditional inactivation of TNFalpha-converting enzyme in chondrocytes results in an elongated growth plate and shorter long bones. PLoS One 8, e54853.
Scaltriti, M., Baselga, J., 2006. The epidermal growth factor receptor pathway: a model for targeted therapy. Clin. Cancer Res. 12, 5268–5272.
Schneider, M.R., Sibilia, M., Erben, R.G., 2009. The EGFR network in bone biology and pathology. Trends Endocrinol. Metab. 20, 517–524.
Seshacharyulu, P., Ponnusamy, M.P., Haridas, D., Jain, M., Ganti, A.K., Batra, S.K., 2012. Targeting the EGFR signaling pathway in cancer therapy. Expert Opin. Ther. Targets 16, 15–31.
Shilo, B.Z., 2003. Signaling by the *Drosophila* epidermal growth factor receptor pathway during development. Exp. Cell Res. 284, 140–149.
Shum, L., Sakakura, Y., Bringas Jr., P., Luo, W., Snead, M.L., Mayo, M., Crohin, C., Millar, S., Werb, Z., Buckley, S., et al., 1993. EGF abrogation-induced fusilli-form dysmorphogenesis of Meckel's cartilage during embryonic mouse mandibular morphogenesis in vitro. Development 118, 903–917.
Sibilia, M., Wagner, B., Hoebertz, A., Elliott, C., Marino, S., Jochum, W., Wagner, E.F., 2003. Mice humanised for the EGF receptor display hypomorphic phenotypes in skin, bone and heart. Development 130, 4515–4525.
Sibilia, M., Kroismayr, R., Lichtenberger, B.M., Natarajan, A., Hecking, M., Holcmann, M., 2007. The epidermal growth factor receptor: from development to tumorigenesis. Differentiation 75, 770–787.
Soltoff, S.P., 2004. Evidence that tyrphostins AG10 and AG18 are mitochondrial uncouplers that alter phosphorylation-dependent cell signaling. J. Biol. Chem. 279, 10910–10918.
Steel, R.G.D., Torrie, J.H., 1996. Analysis of covariance, In: McGraw-Hill (Ed.), Principles and Procedures of Statistics: A Biometrical Approach, 3d edition. ISBN: 9780070610286, pp. 401–437 (New York).
Szende, B., Keri, G., Szegedi, Z., Benedeczky, I., Csikos, A., Orfi, L., Gazit, A., 1995. Tyrphostin induces non-apoptotic programmed cell death in colon tumor cells. Cell Biol. Int. 19, 903–911.
Takeda, H., Inoue, H., Kutsuna, T., Matsushita, N., Takahashi, T., Watanabe, S., Higashiyama, S., Yamamoto, H., 2010. Activation of epidermal growth factor receptor gene is involved in transforming growth factor-beta-mediated fibronectin expression in a chondrocyte progenitor cell line. Int. J. Mol. Med. 25, 593–600.
Tran, T.C., Sneed, B., Haider, J., Blavo, D., White, A., Aiyejorun, T., Baranowski, T.C., Rubinstein, A.L., Doan, T.N., Dingledine, R., Sandberg, E.M., 2007. Automated, quantitative screening assay for antiangiogenic compounds using transgenic zebrafish. Cancer Res. 67, 11386–11392.
Tse, A.C., Ge, W., 2009. Spatial localization of EGF family ligands and receptors in the zebrafish ovarian follicle and their expression profiles during folliculogenesis. Gen. Comp. Endocrinol. 167, 397–407.
Wan, J., Ramachandran, R., Goldman, D., 2012. HB-EGF is necessary and sufficient for Muller glia dedifferentiation and retina regeneration. Dev. Cell 22, 334–347.
Wang, Y., Ge, W., 2004. Cloning of epidermal growth factor (EGF) and EGF receptor from the zebrafish ovary: evidence for EGF as a potential paracrine factor from the oocyte to regulate activin/follistatin system in the follicle cells. Biol. Reprod. 71, 749–760.
Wang, K., Yamamoto, H., Chin, J.R., Werb, Z., Vu, T.H., 2004. Epidermal growth factor receptor-deficient mice have delayed primary endochondral ossification because of defective osteoclast recruitment. J. Biol. Chem. 279, 53848–53856.
Westerfield, M., 2007. THE ZEBRAFISH BOOK, 5th edition. University of Oregon Press, Eugene.
Yarden, Y., Sliwkowski, M.X., 2001. Untangling the ErbB signalling network. Nat. Rev. Mol. Cell Biol. 2, 127–137.
Zeng, F., Singh, A.B., Harris, R.C., 2009. The role of the EGF family of ligands and receptors in renal development, physiology and pathophysiology. Exp. Cell Res. 315, 602–610.
Zhang, X., Siclari, V.A., Lan, S., Zhu, J., Koyama, E., Dupuis, H.L., Enomoto-Iwamoto, M., Beier, F., Qin, L., 2011. The critical role of the epidermal growth factor receptor in endochondral ossification. J. Bone Miner. Res. 26, 2622–2633.
Zhu, J., Shimizu, E., Zhang, X., Partridge, N.C., Qin, L., 2011. EGFR signaling suppresses osteoblast differentiation and inhibits expression of master osteoblastic transcription factors Runx2 and Osterix. J. Cell. Biochem. 112, 1749–1760.